Synthetic and Systems Biotechnology 9 (2024) 609–617

Contents lists available at ScienceDirect

Synthetic and Systems Biotechnology

journal homepage: www.keaipublishing.com/en/journals/synthetic-and-systems-biotechnology

Original Research Article

The LysR family transcriptional regulator ORF-L16 regulates spinosad biosynthesis in *Saccharopolyspora spinosa*

Xin Mu [a], Ru Lei [a], Shuqing Yan [a], Zixin Deng [a,b], Ran Liu [b,c,**], Tiangang Liu [a,b,*]

[a] Key Laboratory of Combinatorial Biosynthesis and Drug Discovery, Ministry of Education and School of Pharmaceutical Sciences, Wuhan University, Wuhan, 430072, Hubei Province, China
[b] State Key Laboratory of Microbial Metabolism, Joint International Research Laboratory of Metabolic and Developmental Sciences, School of Life Sciences and Biotechnology, Shanghai Jiao Tong University, Shanghai, 200030, China
[c] Key Laboratory of Quantitative Synthetic Biology, Shenzhen Institute of Synthetic Biology, Shenzhen Institutes of Advanced Technology, Chinese Academy of Sciences, Shenzhen, 518055, China

ARTICLE INFO

Keywords:
Spinosad
LysR family transcriptional regulator
Spinosyn A
Regulation
Saccharopolyspora spinosa

ABSTRACT

Spinosad, a potent broad-spectrum bioinsecticide produced by *Saccharopolyspora spinosa*, has significant market potential. Despite its effectiveness, the regulatory mechanisms of spinosad biosynthesis remain unclear. Our investigation identified the crucial role of the LysR family transcriptional regulator ORF-L16, located upstream of spinosad biosynthetic genes, in spinosad biosynthesis. Through reverse transcription PCR (RT-PCR) and 5′-rapid amplification of cDNA ends (5′-Race), we unveiled that the spinosad biosynthetic gene cluster (BGC) contains six transcription units and seven promoters. Electrophoretic mobility shift assays (EMSAs) demonstrated that ORF-L16 bound to seven promoters within the spinosad BGC, indicating its involvement in regulating spinosad biosynthesis. Notably, deletion of *ORF-L16* led to a drastic reduction in spinosad production from 1818.73 mg/L to 1.69 mg/L, accompanied by decreased transcription levels of spinosad biosynthetic genes, confirming its positive regulatory function. Additionally, isothermal titration calorimetry (ITC) and EMSA confirmed that spinosyn A, the main product of the spinosad BGC, served as an effector of ORF-L16. Specifically, it decreased the binding affinity between ORF-L16 and spinosad BGC promoters, thus exerting negative feedback regulation on spinosad biosynthesis. This research enhances our comprehension of spinosad biosynthesis regulation and lays the groundwork for future investigations on transcriptional regulators in *S. spinosa*.

1. Introduction

Actinomycetes are known for producing a wide range of bioactive secondary metabolites, such as antibiotics, immunosuppressants, anticancer agents, and insecticides, which are highly valuable in medicine and agriculture [1,2]. Spinosad, a macrolide insecticide derived from *S. spinosa*, exhibits effective insecticidal properties against various pests like mosquitoes, slime parasites, and other lepidopteran pests. Notably, spinosad has minimal toxicity towards mammals, fish, birds, and nontarget insects, making it widely used in agriculture, public health, and medicine [3]. The spinosad BGC, identified in the year 2000, consists of 23 genes [4]. *SpnA*, *spnB*, *spnC*, *spnD*, and *spnE* participate in polyketide chain formation; *spnF*, *spnJ*, *spnL*, and *spnM* contribute to macrolide synthesis; *spnG*, *spnH*, *spnK*, and *spnI* are responsible for rhamnose transfer and methylation; and *spnN*, *spnO*, *spnP*, *spnQ*, *spnS*, and *spnR* are crucial for forosamine synthesis and transfer. Additionally, *gtt*, *gdh*, *epi*, and *kre* are involved in rhamnose synthesis, despite not being within the BGC or its immediate vicinity [5].

The metabolic processes of actinomycetes, such as secondary metabolite production, cell differentiation, and carbon and nitrogen utilization, are crucial for various biological functions. These processes are finely regulated by intricate regulatory systems [6]. Understanding the transcriptional regulators that regulate these processes is essential for harnessing the secondary metabolites produced by actinomycetes.

Peer review under responsibility of KeAi Communications Co., Ltd.
* Corresponding author. Key Laboratory of Combinatorial Biosynthesis and Drug Discovery, Ministry of Education and School of Pharmaceutical Sciences, Wuhan University, Wuhan, 430072, Hubei Province, China.
** Corresponding author. State Key Laboratory of Microbial Metabolism, Joint International Research Laboratory of Metabolic and Developmental Sciences, School of Life Sciences and Biotechnology, Shanghai Jiao Tong University, Shanghai, 200030, China.
E-mail addresses: liuran@whu.edu.cn (R. Liu), liutg@whu.edu.cn (T. Liu).

https://doi.org/10.1016/j.synbio.2024.05.001
Received 4 March 2024; Received in revised form 2 May 2024; Accepted 5 May 2024
Available online 10 May 2024
2405-805X/© 2024 The Authors. Publishing services by Elsevier B.V. on behalf of KeAi Communications Co. Ltd. This is an open access article under the CC BY-NC-ND license (http://creativecommons.org/licenses/by-nc-nd/4.0/).

Secondary metabolite biosynthesis is typically regulated by a complex hierarchy of regulators, including global, pleiotropic, and pathway-specific regulators [7]. Global regulators regulate morphological differentiation and the production of secondary metabolites, while pleiotropic regulators control the production of multiple secondary metabolites. Pathway-specific regulators are responsible for regulating the biosynthesis of individual secondary metabolites and are typically located within or in proximity to secondary metabolite BGCs, such as actII-ORF4 and redD in *S. coelicolor* [8].

Transcriptional regulators in various *Saccharopolyspora* strains have been studied. In *S. spinosa* NRRL18538, the LysR family transcriptional regulator ORF-L16 was knocked out, but spinosad production was not significantly affected [5]. In *S. pogona*, the TetR family transcriptional regulator SP_2845 was found to promote growth and butenyl-spinosyn production by regulating glucose metabolism [9]. Moreover, deletion of the response regulator RegX3 in the SenX3-RegX3 two-component system resulted in enhanced primary metabolism, leading to decreased butenyl-spinosyn production due to insufficient precursors [10]. In *S. erythraea*, the transcriptional regulator BldD was shown to positively regulate erythromycin biosynthesis by binding to erythromycin BGC promoters [11]. However, the transcriptional regulators involved in regulating spinosad biosynthesis in *S. spinosa* remain unidentified.

In this study, we investigated the role of the LysR family transcriptional regulator ORF-L16 on regulating spinosad biosynthesis in the high spinosad-producing *S. spinosa* strain WHU1123. Our findings indicate that ORF-L16 positively regulates spinosad biosynthesis by interacting with spinosad BGC promoters. Furthermore, we observed that spinosyn A, the main product of the spinosad BGC, serves as an effector of ORF-L16. This effector reduces the binding affinity between ORF-L16 and spinosad BGC promoters, leading to a negative feedback regulation on spinosad biosynthesis.

2. Materials and methods

2.1. Strains, plasmids, primers, medium, and culture conditions

The strains, plasmids, and primers used in this study are listed in Tables S1 and S2. *Escherichia. coli* was cultured in LB medium at 37 °C and 220 rpm. For the conjugative transfer of *S. spinosa*, the strains were spread on ABB13 plates (5 g/L soluble starch, 5 g/L soy peptone, 2.1 g/L 3-CN-morpholine propanesulfonic acid, 3 g/L calcium carbonate, 0.01 g/L thiamine hydrochloride, 0.046 g/L ferrous sulfate heptahydrate, 20 g/L agar, pH 7.0) and cultured at 28 °C for 7 d. Then, a 1 cm^2 agar block was picked and cultured in TSB-M medium (30 g/L tryptone soya broth, 50 g/L mannitol) at 220 rpm and 28 °C for 72 h to cultivate the primary seed. The primary seed solution was transferred to the secondary seed by the transfer amount of 2 %, and the secondary seed solution was cultured at 220 rpm and 28 °C for 48 h. The secondary seed solution was transferred to a 50 mL centrifuge tube and centrifuged at 4500 rpm for 10 min to collect the cells. The cells were washed 2–3 times with 20 mL of LB medium, and approximately 5–8 mL of LB medium was added to resuspend the cells for later use. For the fermentation of *S. spinosa*, the strains were spread on 019 plates (5 g/L glucose, 3 g/L yeast extract, 10 g/L enzymatically hydrolyzed casein (N-Z amine type A), 20 g/L agar, pH 7.0) and cultured at 28 °C for 7 d. Then, a 1 cm^2 agar block was picked and cultured in the primary seed (10 g/L glucose, 10 g/L yeast extract, 2 g/L enzymatic casein (N-Z amine type A), 25 g/L cottonseed cake powder, 20 g/L corn starch, 2 g/L magnesium sulfate heptamahydrate, 1 g/L ammonium sulfate, pH 7.0) at 28 °C and 250 rpm for 96 h. The primary seed solution was transferred to the secondary seed by the transfer amount of 1 %, and the secondary seed solution was cultured at 28 °C and 250 rpm for 60 h. The secondary seed solution was transferred to the fermentation medium (80 g/L glucose, 20 g/L cottonseed cake powder, 10 g/L protein powder, 5 g/L yeast powder, 4 g/L trisodium citrate, 2 g/L dipotassium hydrogen phosphate, 3 g/L calcium carbonate, 2 g/L ammonium sulfate, 50 g/L rapeseed oil, pH 7.0) by the transfer amount of 5 %, and the fermentation medium was cultured at 28 °C and 250 rpm for 14 d.

2.2. Construction of the ORF-L16 knockout strain and the ORF-L16 overexpression strain by triparental conjugation

The upstream and downstream fragments of *ORF-L16* were amplified from the WHU1123 genome using the primers Left-arm-F/R and Right-arm-F/R. Then, the two fragments were cloned into the pOJ260 vector to obtain the plasmid pOJ260-Δ*ORF-L16*. The *ORF-L16* gene was amplified from the WHU1123 genome using the primers ORF-L16-pIB139-NdeI and ORF-L16-pIB139-EcoRV. Then, the fragment digested with *Eco*RV and *Nde*I, was cloned into the pIB139 vector to obtain the plasmid pIB139-*ORF-L16*. *E. coli* ET12567/pUB307 and pOJ260-Δ*ORF-L16* in *E. coli* DH10B or pIB139-*ORF-L16* in *E. coli* DH10B were cultured to OD_{600} = 0.6–0.8, and the cells were collected by centrifugation at 3500 rpm for 5 min. The cells were subsequently washed 2–3 times with 20 mL of LB medium. After removing the supernatant, 3–4 mL of LB medium was added to resuspend the cells for later use. The cell suspensions of *S. spinosa* and *E. coli* were mixed in different proportions and spread on ABB13 plates containing 10 mM Mg^{2+}. The plates were incubated at 28 °C for 22 h. For calculations with a solid plate volume of 25 mL, trimethoprim's final concentration of 50 μg/mL and apramycin's final concentration of 15 μg/mL were added to 2 mL of sterile water, which covered the plate. The plates were incubated at 28 °C for 10 d. The *ORF-L16* deletion strain was screened for continuous cell culture: the conjugant did not grow on the resistant plate and grew on the nonresistant plate at the same time, suggesting that the conjugant could be a strain with gene knockout. The candidate conjugants were expanding cultured, and the genome was subsequently extracted for verification using the primers F1–F/R. The screening of the *ORF-L16* overexpression strain did not require continuous cell culture. The conjugants were expanding cultured, and the genome was subsequently extracted and verified using the primers Apr-F/R.

2.3. Purification of ORF-L16

The *ORF-L16* gene was amplified from the WHU1123 genome using the primers ORF-L16-HindIII and ORF-L16-NdeI, and the fragment digested with *Hin*dIII and *Nde*I was cloned into the pET28a vector to obtain the plasmid pET28a-*ORF-L16*. The pET28a-*ORF-L16* plasmid was transformed into *E. coli* BL21(DE3) to obtain the recombinant strain BL21(DE3)-*ORF-L16*. The strain was cultured to OD_{600} = 0.6–0.8 and induced by adding 100 mM IPTG at 18 °C for approximately 20 h. The cells were collected by centrifugation at 6000 rpm for 10 min at 4 °C. Subsequently, the cells were resuspended in buffer A containing 10 mM imidazole (50 mM Tris-Cl (pH 7.6), 300 mM NaCl, and 4 mM β-mercaptoethanol). The cell suspensions were lysed using a high-pressure homogenizer, and the supernatant was collected by centrifugation at 10,000 rpm for 1 h at 4 °C. Then, the supernatant was added to Ni-NTA sepharose equilibrated with buffer A containing 10 mM imidazole. The unbound proteins were washed off with 30 times the column volume of buffer A containing 10 mM imidazole. The nonspecific binding proteins were washed off with 20 times the column volume of buffer A containing 30 mM imidazole, 15 times the column volume of buffer A containing 60 mM imidazole, and 10 times the column volume of buffer A containing 90 mM imidazole. Finally, the target protein was eluted using 5 times the column volume of buffer A containing 300 mM imidazole. The target protein was concentrated using a 10 kDa ultrafiltration tube and preserved in protein storage buffer (50 mM Tris, 100 mM NaCl, and 10 % glycerol, pH 8.0).

2.4. Electrophoretic mobility shift assay

FAM-labeled promoters were amplified from the WHU1123 genome using the FAM-labeled primers listed in Table S2, and unlabeled

promoters were amplified from the WHU1123 genome using the unlabeled primers listed in Table S2. The nonspecific fragment poly(dI-dC) was purchased from Merck. Reaction system: 10 μL of 2 × binding buffer (4 mM Tris, 12 mM 4-hydroxyethyl piperazine ethanesulfonic acid, 60 mM potassium chloride, 0.5 mM ethylene diamine tetraacetic acid, 5 mM Mg^{2+}, 1 mM dithiothreitol, 0.4 mM 2-oxoglutarate, 20 % glycerol, pH 8.0), 10 ng of FAM-labeled promoter, 100–400 nM ORF-L16 protein, and ddH_2O were added to a final volume of 20 μL. Electrophoresis was performed after 20 min of reaction at room temperature. Subsequent imaging was performed using the Alex488 program of the Bio-Rad imaging system.

2.5. ITC analysis

Microcal ITC (Malvern Panalytical) was used for isothermal titration calorimetric studies. The sample cell was filled with a 30 μM solution of ORF-L16 protein. To initiate the titration, the syringe was used to inject 100 μM of spinosyn A, dissolved in protein storage buffer. The stirring speed and reaction temperature were set at 750 rpm and 30 °C, respectively. Additionally, as a control for background, spinosyn A solution was injected into the protein storage buffer without any protein present. The integrated heats from each titration were fitted to a single-site binding isotherm and normalized to the moles of ligand per titration using Microcal PEAQ-ITC Analysis Software version 1.41.

2.6. RNA extraction and RT-PCR

Total RNA was extracted from the WHU1123 strain during the mid-logarithmic phase of fermentation. The cells in the mid-logarithmic phase were collected by centrifugation at 6000 rpm for 6 min at 4 °C and washed twice with ddH_2O. The cells were divided into approximately 100 mg per portion, frozen in liquid nitrogen, and stored at −80 °C. Total RNA was extracted according to the instructions of the RNA Extraction Plant Mini Kit (QIAGEN). The PrimeScript RT Reagent Kit with gDNA Eraser (Takara) was used for DNA removal and reverse transcription, and cDNA was used as a template to verify the transcription unit of the spinosad BGC using the primers listed in Table S2. The PCR products were subsequently sequenced.

2.7. 5′-Race analysis

The 5′-Race technique was used to amplify the 5′ end of the putative transcription unit. After RNA extraction, we amplified cDNA with the HiScript-TS 5′/3′ RACE Kit (Vazyme) using the primers in Table S2. The PCR products were cloned into the pCE3 vector and transformed into *E. coli* DH10B. The plasmids were extracted and sequenced, and the transcription start site was determined by alignment of the sequencing sequence with the genome sequence.

2.8. Detection of spinosad production

At the end of fermentation, 4 mL of ethanol was added to 1 mL of fermentation broth. The mixture was sonicated for 10 min and vortexed for 10 min. Subsequently, centrifugation at 8000 rpm for 10 min was performed to obtain the supernatant. The supernatant was filtered through a 0.22 μM microporous filter membrane. The HPLC detection method was as follows: mobile phase, methanol: acetonitrile: water (containing 5 % ammonium acetate) = 45:45:10; flow rate, 1 mL/min; detection wavelength: 250 nm; and column temperature: 30 °C. The spinosad productions of the strains were determined by comparison with the standard spinosyn A and spinosyn D.

2.9. AlphaFold2 prediction and molecular docking analysis

AutoDock Vina [12] (version 1.1.2) was used for molecular docking analysis. Before the docking procedure, the receptor structure predicted by AlphaFold2 [13] and the ligand were processed as follows. The acceptor was subjected to water removal and hydrogenation, and the ligand was subjected to hydrogenation. The grid box in the docking procedure was defined to include the effector binding domain at the C-terminus of the acceptor, and the corresponding residues appeared in the binding site of the crystal structure. The receptor and ligand options in AutoDock Vina were set to the defaults. The number of binding modes, exhaustiveness of the search, and maximum energy difference (kcal/mol) parameters were set as 9, 8, and 3, respectively.

3. Results

3.1. ORF-L16, a LysR family transcriptional regulator

The transcriptional regulators of secondary metabolites are crucial for understanding and utilizing those compounds. The genes involved in spinosad biosynthesis have been identified, except for the accessory protein of SpnP [14]. However, the transcriptional regulators for spinosad biosynthesis have not yet been reported. Typically, pathway-specific regulators for secondary metabolites are located near the corresponding BGCs. Therefore, we conducted a BLAST analysis on the genes upstream and downstream of spinosad biosynthetic genes. *ORF-L15* and *ORF-L16*, located upstream, were predicted to encode a ketoacyl reductase and a LysR family transcriptional regulator, respectively. On the other hand, *ORF-R1* and *ORF-R2*, downstream genes, were predicted to encode a protein with a DUF4232 domain of unknown function and an exodeoxyribonuclease V, respectively (Fig. 1A). Notably, the LysR family transcriptional regulator ORF-L16, with 837 nucleotides and encoding 278 amino acids, is a potential regulator in regulating spinosad biosynthesis.

LysR family transcriptional regulators are widely distributed among bacteria, archaea, and algae. These regulators typically contain a conserved HTH-DNA binding domain (DBD) at the N-terminus and an effector binding domain (EBD) at the C-terminus. The DBD specifically binds to the promoter region of target genes, and the EBD interacts with effectors to regulate target gene expression. LysR family transcriptional regulators lay a role in various physiological processes such as central carbon metabolism, amino acid biosynthesis, cell division, and secondary metabolite production [15]. Notably, multiple amino acid sequence alignment showed that the DBD of ORF-L16 shares 56 % identity with the DBDs of LysR family transcriptional regulators that have complete crystal structures (Fig. 1B). Based on this finding, we hypothesized that ORF-L16 may interact with spinosad BGC promoters.

3.2. Characteristics of the transcription units and transcription start sites within the spinosad BGC

In prokaryotes, mRNA is typically found in a polycistronic structure where one polycistron serves as a transcription unit. To investigate the transcriptional units of the spinosad BGC, total RNA was extracted from the WHU1123 strain. Primers were then designed based on gene transcription patterns, and RT-PCR was conducted. Our findings indicated the presence of six transcription units: *spnQ-spnS*, *spnP-spnN*, *spnJ-spnM*, *spnI*, *spnG-spnH*, and *spnF-spnE*. The largest transcription unit, *spnF-spnE*, contained six genes spanning about 56 kb (Fig. 2A and B). This suggests that the spinosad BGC contains at least six promoters located upstream of the *spnQ*, *spnP*, *spnJ*, *spnI*, *spnG*, and *spnF*. However, Tan et al. previously reported 14 post-modified genes within the spinosad BGC of *S. albus* 1074, which showed heterogeneous expression of the spinosad BGC, grouped into eight transcription units [16]. Song et al. discovered that five polyketide synthase genes within the spinosad BGC of *S. albus* 1074, which heterogeneously expressed the spinosad BGC, formed two transcription units [17]. Combining these finding, it can be inferred that the spinosad BGC in *S. albus* 1074 contains ten transcription units. We propose that this difference may be due to discrepancies in the host systems.

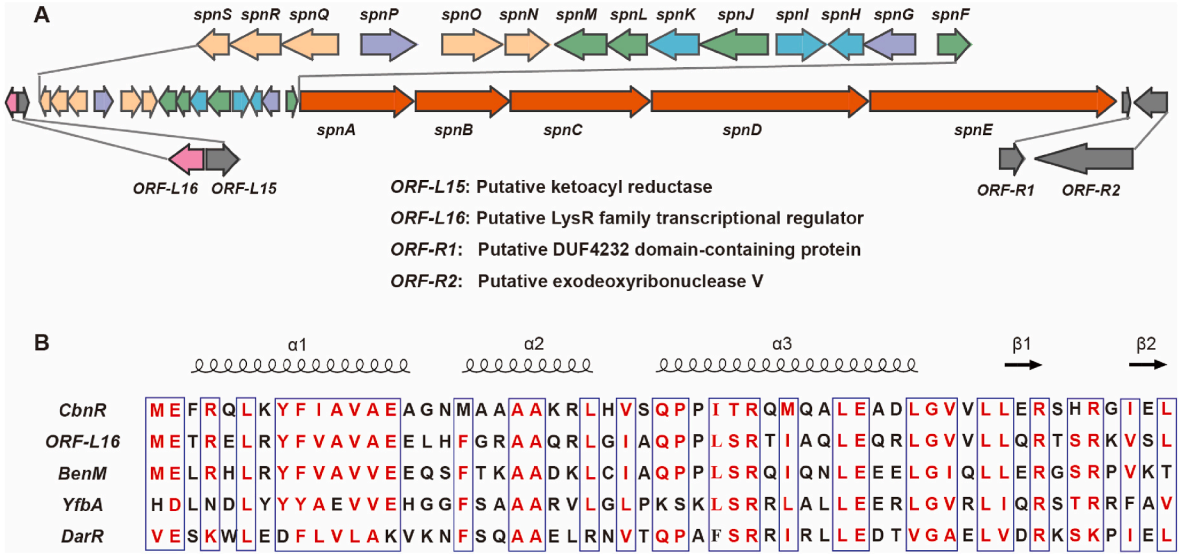

Fig. 1. Analysis of the upstream and downstream genes of spinosad biosynthetic genes. (A) BLAST analysis of the upstream and downstream genes of spinosad biosynthetic genes. (B) Multiple amino acid sequence alignment of the DBDs of the ORF-L16 and LysR family transcriptional regulators with complete crystal structures. CbnR is from *Burkholderiales* [30], BenM is from *Acinetobacter* [37], YfbA is from *Yersinia pestis*, and DarR is from *Aliivibrio fischeri* [38].

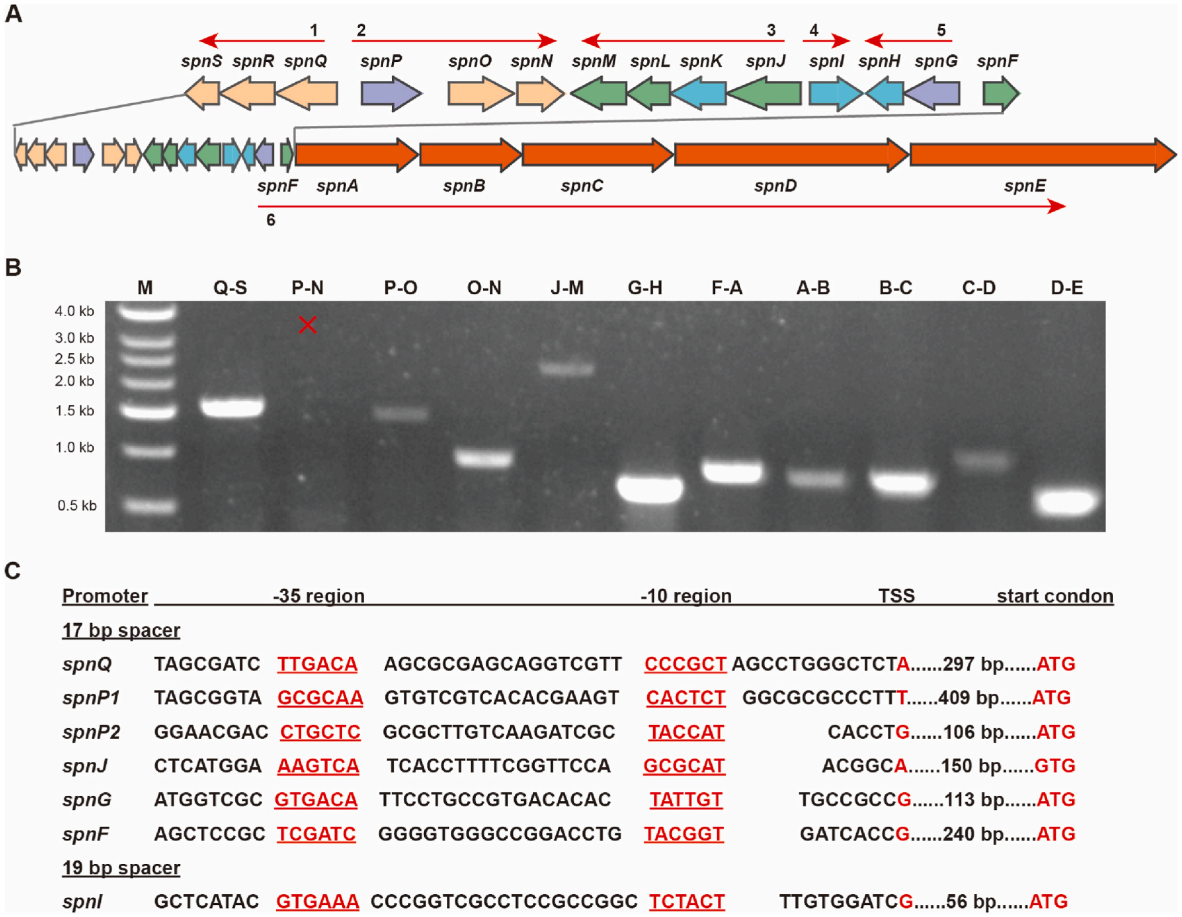

Fig. 2. The transcription units and TSSs of the spinosad BGC. (A) The transcription units of the spinosad BGC were analyzed by RT-PCR. (B) Gel electrophoresis of RT-PCR products. (C) 5′-Race was used to characterize the TSSs of the six transcription units within the spinosad BGC, and the −35 region and −10 region of the seven promoters as well as the interval between these two regions were inferred.

To delineate the spinosad BGC promoter regions, we utilized the 5′-Race technique to identify the transcription start sites (TSSs) of the six transcription units. Our findings revealed that the TSS of the *spnQ* promoter was located at an adenine (A), −297 bp from the *spnQ* start codon. For the *spnP-spnN* transcriptional unit, two TSSs were identified: a thymidine (T), −409 bp from the *spnP* start codon and a guanine (G),

−106 bp relative to the *spnP* start codon, indicating the presence of dual promoters. Interestingly, similar to the erythromycin BGC, where genes like *ermE* and *eryCI* also exhibit two TSSs [18], it seems common for genes to be regulated by multiple promoters. The TSS of the *spnJ* promoter was found at an adenine (A), −150 bp from the *spnJ* start codon; the *spnI* promoter's TSS was identified at a guanine (G), −56 bp from the *spnI* start codon; the TSS of the *spnG* promoter was located at a guanine (G), −113 bp from the *spnG* start codon; and the TSS of the *spnF* promoter was positioned at a guanine (G), −240 bp from the *spnF* start codon (Fig. 2C). These results enhance our understanding of the complex transcriptional regulatory mechanisms regulating the spinosad biosynthetic pathway. The majority of the seven TSSs were purines and situated more than 100 bp from the start codon, indicating the presence of a 5′-untranslated region (5′-UTR) preceding the start codon.

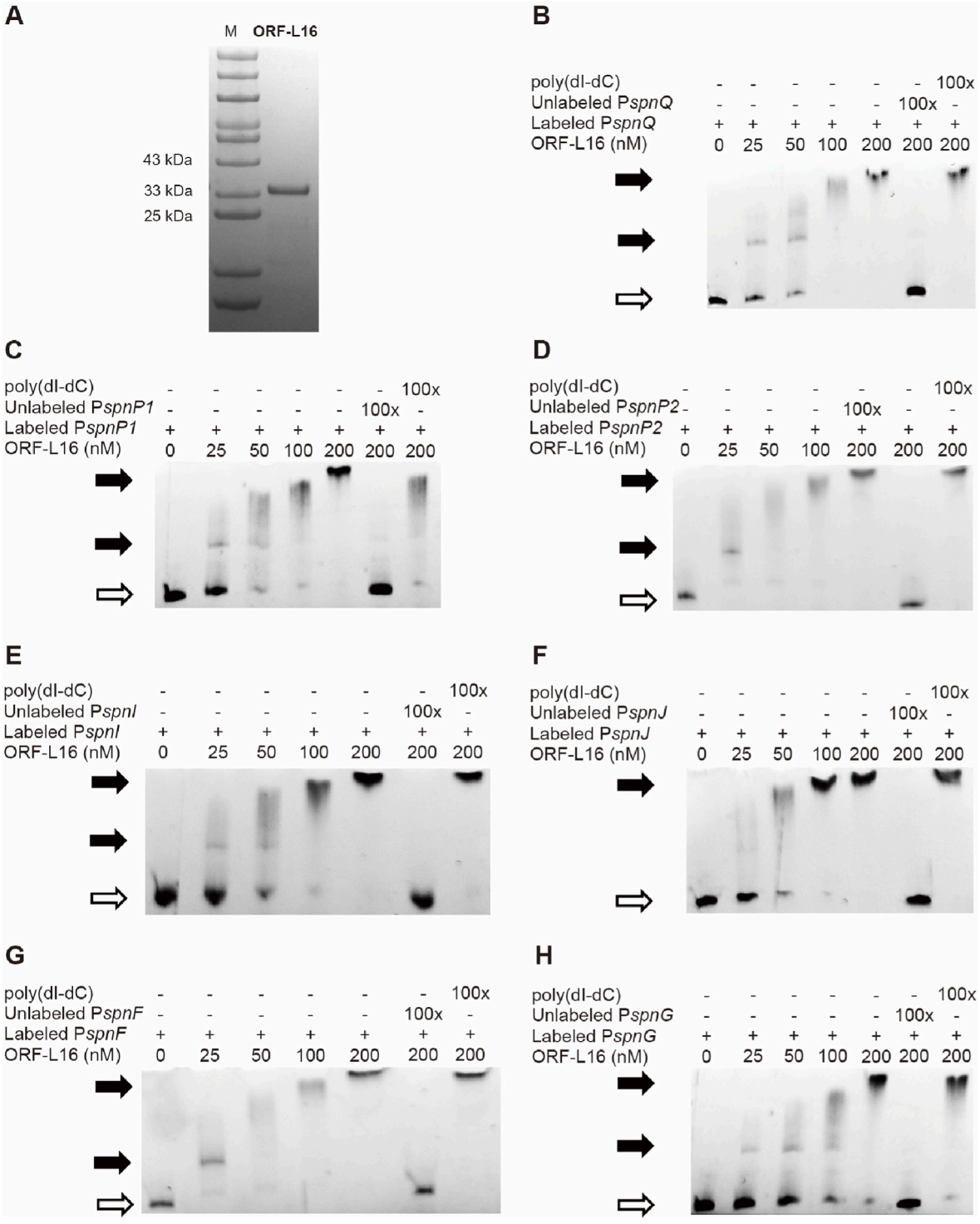

Fig. 3. EMSAs of spinosad BGC promoters and ORF-L16. (A) SDS-PAGE electrophoresis of the ORF-L16 protein. The (B) *spnQ* promoter, (C) *spnP1* promoter, (D) *spnP2* promoter, (E) *spnI* promoter, (F) *spnJ* promoter, (G) *spnF* promoter, and (H) *spnG* promoter interacted with the ORF-L16 protein in a concentration-dependent and specific manner. Hollow arrows indicated the free promoter, solid arrows indicated the complex of the promoter and protein. The EMSA results are representative examples of three independent experiments.

Alterations in the secondary structure of the 5′-UTR, a *cis*-acting RNA element, can impact transcription attenuation, transcript stability, and the accessibility of ribosome binding sites, thereby influencing gene expression [19]. Consequently, the transcription of spinosad BGC may be regulated at the posttranscriptional level, influenced by the characteristics of the 5′-UTR.

Prokaryotic promoters usually contain the −35 region and −10 region, which are crucial for the recognition and binding of RNA polymerases [20]. In *Streptomyces* promoters, the TTGAC (Pu) and TAg (Pu) (Pu) T sequences are conserved in the −35 region and −10 region, respectively. Notably, the guanine (G) at the third position in the −35 region and the thymidine (T) at the sixth position in the −10 region are completely conserved (100 %) [21]. This conservation pattern was used to infer the −35 region and −10 region of the spinosad BGC promoters (Fig. 2C). The optimal distance between the −35 region and −10 region in prokaryotic promoters is usually 16 to 19 bp, highlighting the importance of proper spacing for promoter activity [20]. In the spinosad BGC promoters, the distance between the predicted −35 region and −10 region was 17 bp and 19 bp (Fig. 2C).

3.3. ORF-L16 interacts with spinosad BGC promoters

After identifying spinosad BGC promoter regions, we purified the ORF-L16 protein (Fig. 3A) and conducted EMSAs to explore the interaction between the promoters and ORF-L16. Our findings showed that with increasing concentrations of ORF-L16, the concentration of the free FAM-labeled *spnQ* promoter decreased. The *spnQ* promoter displayed a concentration-dependent binding to ORF-L16. In competitive experiment, upon the introduction of a 100-fold excess of the unlabeled *spnQ* promoter, the FAM-labeled *spnQ* promoter exhibited no displacement. In specificity experiment, the presence of a 100-fold excess of the nonspecific fragment poly(dI-dC) did not affect ORF-L16 binding to the FAM-labeled *spnQ* promoter (Fig. 3B). Further analysis of the other six promoters showed displacement patterns that were comparable to those observed for the *spnQ* promoter (Fig. 3C–H). These results suggest that ORF-L16 specifically interacts with all seven promoters within the spinosad BGC, indicating a regulatory role in spinosad biosynthesis.

3.4. Effects of ORF-L16 deletion and overexpression on spinosad biosynthesis

To investigate the role of ORF-L16 in regulating spinosad biosynthesis, a pOJ260-Δ*ORF-L16* plasmid was designed to knockout the *ORF-L16*. Upon introducing this plasmid into the WHU1123 strain, a strain labeled Δ*ORF-L16* was obtained (Fig. S1A). HPLC analysis showed a significant decrease in spinosad production from 1818.73 mg/L to 1.69 mg/L in the Δ*ORF-L16* strain (Fig. 4A). Subsequently, total RNA was extracted from both the Δ*ORF-L16* and WHU1123 strains to assess the transcription levels of spinosad biosynthetic genes. RNA sequencing revealed downregulation of these genes in the Δ*ORF-L16* strain (Fig. 4B). These findings suggest a positive regulatory role of ORF-L16 in spinosad biosynthesis.

The upregulation of positive transcriptional regulators commonly enhances the production of secondary metabolites. For instance, when the positive transcriptional regulator FkbR1 was overexpressed in *S. hygroscopicus* var. ascomyceticus ATCC 14891, there was a 33.5 % increase in ascomycin production [22]. To enhance spinosad production, a site-integrated plasmid pIB39-*ORF-L16* was constructed with the *ermEp** promoter for *ORF-L16* overexpression. When introduced into the WHU1123 strain, the resulting strain, designated OE-*ORF-16* (Fig. S1B), showed a 51.8 % reduction in spinosad production (Fig. 4A). This phenomenon of decreased secondary metabolite production upon overexpression of positive transcriptional regulators is not unique to spinosad biosynthesis and has been observed in other systems. For instance, Liu et al. observed about 40 % decrease in avermectin production when *aveR*, a positive regulator, was overexpressed via the low-copy vector in *S. avermectin* K139. The delicate balance required for optimal regulation was highlighted by the inability to obtain transformants when *aveR* was overexpressed using a high-copy vector [23]. Additionally, He et al. introduced geldanamin's positive transcriptional regulators into corresponding knockout strains using PSG5-derived vectors (with a copy number of 20–50). However, this supplementation only restored geldanamin production to about 30 % of wild-type level [24]. In contract, Wilson et al. successfully restored *pik* BGC product yields to wild-type levels by supplementing *pikD*, the positive regulator, using a low-copy vector [25]. These results suggest that some positive regulators may not consistently improve production within their host and that there may be an intracellular threshold concentration

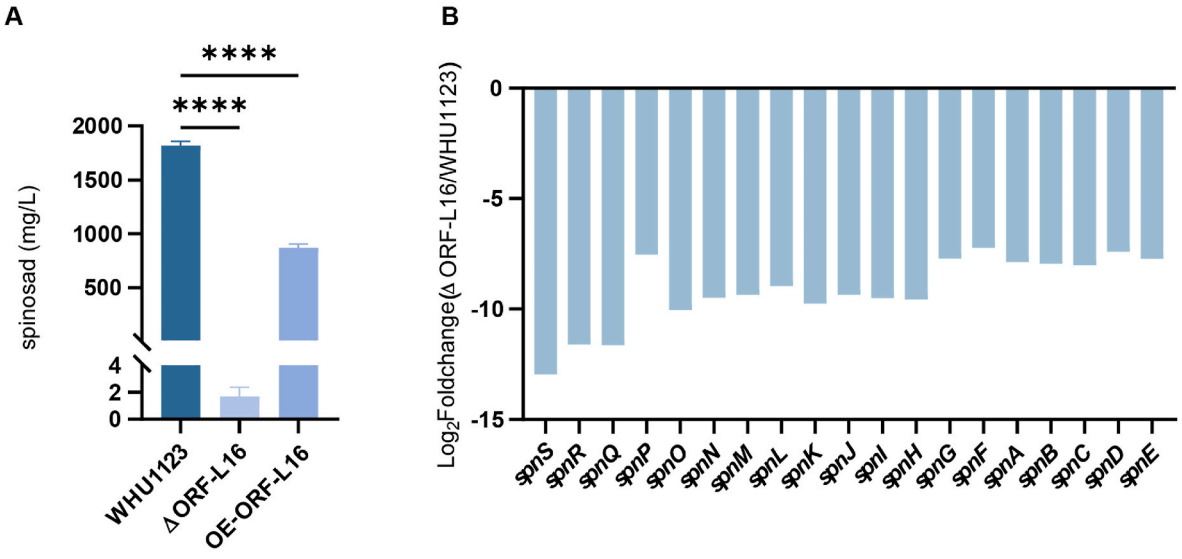

Fig. 4. Effects of *ORF-L16* deletion and overexpression on spinosad production. (A) Spinosad productions of engineered strains with deletion and overexpression *ORF-L16* and the control strain WHU1123. Error bars are standard deviations from three independent experiments, and *P* values were tested by Student's *t*-test. ****, $P \leq 0.0001$. (B) Logarithmic transformation of the transcriptional level ratio between the Δ*ORF-L16* and WHU1123 strains for spinosad biosynthetic genes. RNA sequencing was conducted in three independent experiments, and the *P* values are shown in Table S3.

beyond which abnormal effects occur. Therefore, it is hypothesized that ORF-L16 may also function within such a threshold concentration in the WHU1123 strain.

3.5. Spinosyn A affects the interaction between ORF-L16 and spinosad BGC promoters

It is widely acknowledged that secondary metabolites [26] or biosynthetic intermediates [27] act as effectors to regulate their biosynthesis in actinomycetes. In addition, Wu et al. showed that propionyl-CoA and methylmalonyl-CoA, direct precursors of erythromycin, act as effectors to regulate erythromycin biosynthesis in *S. erythraea* [28]. Given that ORF-L16 positively regulates spinosad biosynthesis, we hypothesized that a product or intermediate from the spinosad biosynthesis pathway could potentially act as an effector of ORF-L16. To explore this hypothesis, we conducted molecular docking studies involving three compounds: spinosyn A (the main product of the spinosad BGC), aglycone, and pseudoaglycone (two representative intermediates), with ORF-L16. Firstly, we utilized AlphaFold2 to predict the structure of ORF-16 (Fig. S2), which exhibited the typical architecture of LysR family transcriptional regulators, with a high per-residue LDDT (pLDDT) score of 92.067. Secondly, molecular docking simulations using AutoDock Vina software revealed an affinity of −9.2 kcal/mol between ORF-L16 and spinosyn A (Fig. 5A). Additionally, interactions between ORF-L16 and aglycone, as well as pseudoaglycone, exhibited affinities of −8.7 kcal/mol and −8.3 kcal/mol, respectively (Fig. S3). Notably, the observed hydrogen bonding patterns in these interactions suggest the potential effector role of these compounds on ORF-L16. While all three compounds could potentially act as effectors, spinosyn A demonstrated a stronger affinity with ORF-L16, indicating it is more likely to be considered as ORF-L16's effector. Thirdly, the dissociation constant (Kd) for the spinosyn A-ORF-L16 interaction was determined to be 2.36 ± 0.04 μM using ITC (Fig. 5C and D), thereby confirming spinosyn A as the effector of ORF-L16.

The binding of effectors could influence the interaction between transcriptional regulators and DNA [27]. To investigate this, we conducted EMSA using spinosyn A, and DMSO as a negative control. When spinosyn A was add, the free *spnQ* promoter was observed, indicating that spinosyn A reduced the affinity of ORF-L16 for the *spnQ* promoter (Fig. 5B). This result suggest that spinosyn A negatively regulates spinosad biosynthesis through feedback mechanism, ultimately affecting spinosad production in the WHU1123 strain.

4. Discussion

This study showed that ORF-L16, a member of LysR family transcriptional regulators, plays a positive role in regulating spinosad biosynthesis in the WHU1123 strain. Additionally, spinosyn A was found to exert negative feedback regulation on spinosad biosynthesis. It is noteworthy that this study represents the first report of a transcriptional regulator involved spinosad biosynthesis.

Transcriptional regulators play diverse roles depending on the presence of different effectors. For instance, the LysR family transcriptional regulator CysB regulates cysteine biosynthesis in bacteria. N-acetylserine serves as an inducer, activating CysB's transcriptional regulation, while thiosulfate acts as an anti-inducer, inhibiting CysB-mediated regulation [29]. This study identified spinosyn A as an anti-inducer of ORF-L16, however, the inducer of ORF-L16 remains

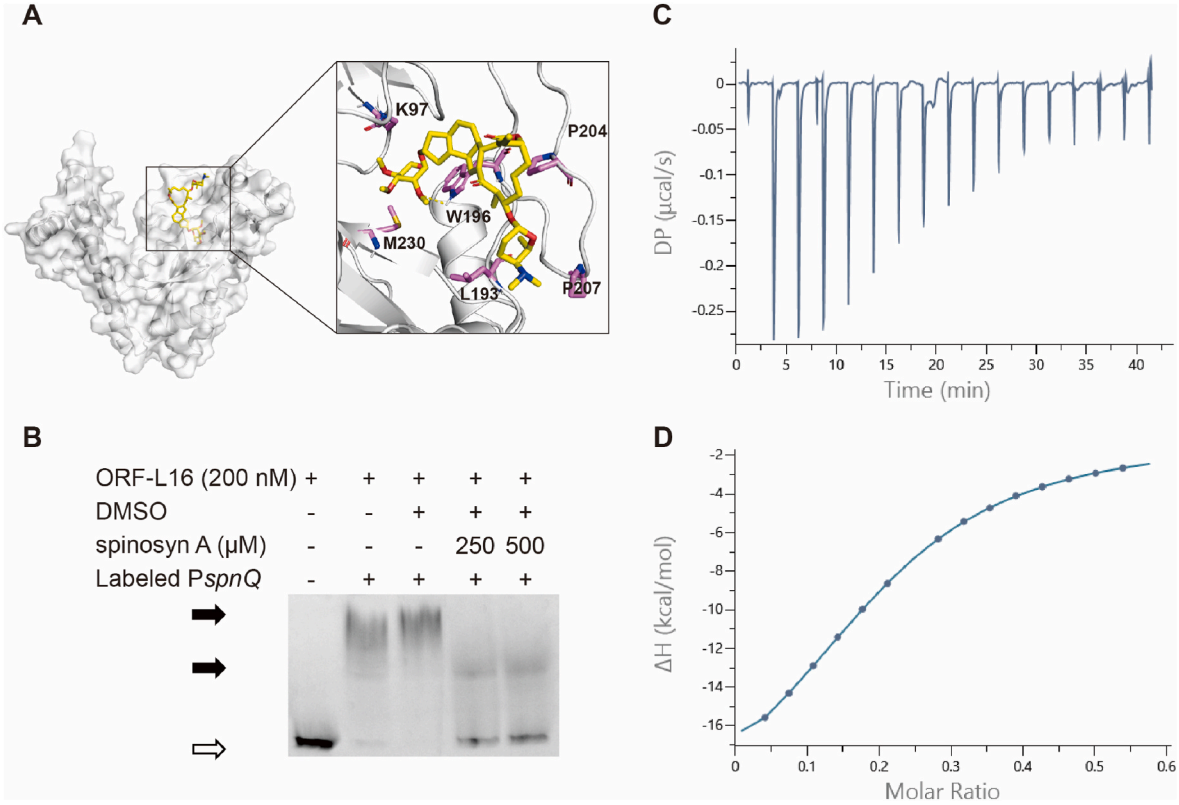

Fig. 5. The interaction between spinosyn A and ORF-L16. (A) AutoDock Vina was used to simulate the molecular docking of the predicted ORF-L16 protein structure and spinosyn A. The NH of tryptophan indole group at position 196 in ORF-L16 formed a hydrogen bond with the oxygen atom in the 2′-methoxy group of spinosyn A rhamnose, with a distance of 2.8 Å. (B) Effect of spinosyn A on interaction between ORF-L16 and the *spnQ* promoter. Hollow arrows indicated the free promoter, solid arrows indicated the complex of the promoter and protein. The EMSA result is the representative example of three independent experiments. (C) ITC curve of the interaction of ORF-L16 with spinosyn A at 30 °C. The integrated injection heats derived from the titrations, corrected for control dilution heat. (D) The solid line is the best-fit curve and was used to derive the binding parameter.

unknown. Positive regulation by LysR family transcriptional regulators requires inducers that bind to regulators, forming complexes that interact with the α-CTD domain of RNA polymerases. This interaction enhances RNA polymerase binding affinity to the promoter, initiating transcription [30]. Deletion of *ORF-L16* in the NRRL18538 strain did not significantly impact spinosad production [5], but in the WHU1123 strain, spinosad production was significantly reduced. Two possible reasons for this difference were proposed: 1) NRRL18538, a wild-type strain with inherently low yield characteristics, exhibited minimal effects upon *ORF-L16* knockout. 2) In NRRL18538, the inducer concentration required to activate ORF-L16's positive regulatory effect may be insufficient, leading to non-significant effects upon *ORF-L16* knockout. Conversely, in the WHU1123 strain, moderate to high inducer concentrations effectively activated ORF-L16's positive regulatory effect. Interestingly, Tcs7, a LysR family transcriptional regulator, positively regulates FK506 biosynthesis in *S. tsukubaensis* L19, but negatively regulates FK506 biosynthesis in *S.* sp. KCTC11604BP [31]. These results indicate that the same regulator may have different regulatory roles in different strains, potentially influenced by the concentration of the effector. In future studies, a differential scanning fluorescence (DSF) assay [32] may aid in identifying the inducers of ORF-L16.

In the synthesis of secondary metabolites, both the intermediate and end product can act as effectors of transcriptional regulators, regulating the synthesis of secondary metabolites. For instance, jadomycin B and its biosynthetic intermediates (2,3-dehydro-UWM6, dehydrorabelomycin, and jadomycin A) have been showed to influence the DNA binding ability of JadR*. Among these, dehydrorabelomycin had the most significant dissociation effect [33]. Similarly, in *S. antibioticus*, chloramphenicol and its biosynthetic intermediates (demethylsalicycloyl chlorothricin and deschloro-chlorothricin) act as effectors, regulating the binding of ChlF1* to target genes [34]. These findings suggest that investigating the relationship between intermediates such as aglycone and pseudoaglycone with ORF-L16 could enhance our understanding of the regulatory mechanisms involving ORF-L16.

This study serves as a foundational exploration into the regulation of spinosad biosynthesis. The complex mechanism that generates secondary metabolites in actinomycetes involves factors such as small signaling molecules [35] and the hierarchy of transcriptional proteins [36]. Understanding how ORF-L16 collaborates with these factors would facilitate the development of novel strategies for strain improvement.

CRediT authorship contribution statement

Xin Mu: Methodology, Investigation, Writing – original draft. **Ru Lei:** Investigation. **Shuqing Yan:** Investigation. **Zixin Deng:** Conceptualization, Supervision. **Ran Liu:** Conceptualization, Investigation, Writing – review & editing, Supervision, Project administration, Funding acquisition. **Tiangang Liu:** Conceptualization, Investigation, Writing – review & editing, Supervision, Project administration, Funding acquisition.

Declaration of competing interest

The authors applied a patent based on this research.

Zixin Deng and Tiangang Liu are Founding Editor and Editorial Board Member for Synthetic and Systems Biotechnology, respectively. And they were not involved in the editorial review or the decision to publish this article.

Acknowledgment

This work was supported by the National Key R&D Program of China (grant number 2018YFA0900400), the National Natural Science Foundation of China (grant number 32100053), and the Young Elite Scientists Sponsorship Program by China Association for Science and Technology (grant number YESS20210068).

Appendix A. Supplementary data

Supplementary data to this article can be found online at https://doi.org/10.1016/j.synbio.2024.05.001.

References

[1] Chater KF. *Streptomyces* inside-out: a new perspective on the bacteria that provide us with antibiotics. Philos Trans R Soc Lond B Biol Sci 2006;361:761–8. https://doi.org/10.1098/rstb.2005.1758.
[2] Zhang L, Demain A. Natural products: drug discovery and therapeutic medicine. 2005.
[3] Santos VSV, Pereira BB. Properties, toxicity and current applications of the biolarvicide spinosad. J Toxicol Environ Health B Crit Rev 2020;23:13–26. https://doi.org/10.1080/10937404.2019.1689878.
[4] Waldron C, Madduri K, Crawford K, Merlo DJ, Treadway P, Broughton MC, et al. A cluster of genes for the biosynthesis of spinosyns, novel macrolide insect control agents produced by *Saccharopolyspora spinosa*. Antonie Leeuwenhoek 2000;78:385–90. https://doi.org/10.1023/a:1010289901631.
[5] Waldron C, Matsushima P, Rosteck Jr PR, Broughton MC, Turner J, Madduri K, et al. Cloning and analysis of the spinosad biosynthetic gene cluster of *Saccharopolyspora spinosa*. Chem Biol 2001;8:487–99. https://doi.org/10.1016/s1074-5521(01)00029-1.
[6] Romero-Rodríguez A, Robledo-Casados I, Sánchez S. An overview on transcriptional regulators in *Streptomyces*. Biochim Biophys Acta 2015;1849:1017–39. https://doi.org/10.1016/j.bbagrm.2015.06.007.
[7] Chen Y, Wendt-Pienkowski E, Shen B. Identification and utility of FdmR1 as a *Streptomyces* antibiotic regulatory protein activator for fredericamycin production in *Streptomyces griseus* ATCC 49344 and heterologous hosts. J Bacteriol 2008;190:5587–96. https://doi.org/10.1128/jb.00592-08.
[8] Fujii T, Gramajo HC, Takano E, Bibb MJ. *redD* and *act*II-ORF4, pathway-specific regulatory genes for antibiotic production in *Streptomyces coelicolor* A3(2), are transcribed in vitro by an RNA polymerase holoenzyme containing sigma *hrdD*. J Bacteriol 1996;178:3402–5. https://doi.org/10.1128/jb.178.11.3402-3405.1996.
[9] Rang J, Xia Z, Shuai L, Cao L, Liu Y, Li X, et al. A TetR family transcriptional regulator, SP_2854 can affect the butenyl-spinosyn biosynthesis by regulating glucose metabolism in *Saccharopolyspora pogona*. Microb Cell Factories 2022;21:83. https://doi.org/10.1186/s12934-022-01808-2.
[10] Rang J, He H, Chen J, Hu J, Tang J, Liu Z, et al. SenX3-RegX3, an important two-component system, regulates strain growth and butenyl-spinosyn biosynthesis in *Saccharopolyspora pogona*. iScience 2020;23:101398. https://doi.org/10.1016/j.isci.2020.101398.
[11] Chng C, Lum AM, Vroom JA, Kao CM. A key developmental regulator controls the synthesis of the antibiotic erythromycin in *Saccharopolyspora erythraea*. Proc Natl Acad Sci USA 2008;105:11346–51. https://doi.org/10.1073/pnas.0803622105.
[12] Trott O, Olson AJ. AutoDock Vina: improving the speed and accuracy of docking with a new scoring function, efficient optimization, and multithreading. J Comput Chem 2010;31:455–61. https://doi.org/10.1002/jcc.21334.
[13] Jumper J, Evans R, Pritzel A, Green T, Figurnov M, Ronneberger O, et al. Highly accurate protein structure prediction with AlphaFold. Nature 2021;596:583–9. https://doi.org/10.1038/s41586-021-03819-2.
[14] Isiorho EA, Jeon BS, Kim NH, Liu HW, Keatinge-Clay AT. Structural studies of the spinosyn forosaminyltransferase, SpnP. Biochemistry 2014;53:4292–301. https://doi.org/10.1021/bi5003629.
[15] Mayo-Pérez S, Gama-Martínez Y, Dávila S, Rivera N, Hernández-Lucas I. LysR-type transcriptional regulators: state of the art. Crit Rev Microbiol 2023:1–33. https://doi.org/10.1080/1040841x.2023.2247477.
[16] Tan G-Y, Deng K, Liu X, Tao H, Chang Y, Chen J, et al. Heterologous biosynthesis of spinosad: an omics-guided large polyketide synthase gene cluster reconstitution in *Streptomyces*. ACS Synth Biol 2017;6:995–1005. https://doi.org/10.1021/acssynbio.6b00330.
[17] Song C, Luan J, Cui Q, Duan Q, Li Z, Gao Y, et al. Enhanced heterologous spinosad production from a 79-kb synthetic multioperon assembly. ACS Synth Biol 2019;8:137–47. https://doi.org/10.1021/acssynbio.8b00402.
[18] Reeves AR, English RS, Lampel JS, Post DA, Vanden Boom TJ. Transcriptional organization of the erythromycin biosynthetic gene cluster of *Saccharopolyspora erythraea*. J Bacteriol 1999;181:7098–106. https://doi.org/10.1128/jb.181.22.7098-7106.1999.
[19] Adams PP, Baniulyte G, Esnault C, Chegireddy K, Singh N, Monge M, et al. Regulatory roles of *Escherichia coli* 5' UTR and ORF-internal RNAs detected by 3' end mapping. Elife 2021;10. https://doi.org/10.7554/eLife.62438.
[20] Turecka K, Firczuk M, Werel W. Alteration of the -35 and -10 sequences and deletion the upstream sequence of the -35 region of the promoter A1 of the phage T7 in dsDNA confirm the contribution of non-specific interactions with *E. coli* RNA polymerase to the transcription initiation process. Front Mol Biosci 2023;10:1335409. https://doi.org/10.3389/fmolb.2023.1335409.
[21] Strohl WR. Compilation and analysis of DNA sequences associated with apparent streptomycete promoters. Nucleic Acids Res 1992;20:961–74. https://doi.org/10.1093/nar/20.5.961.
[22] Song K, Wei L, Liu J, Wang J, Qi H, Wen J. Engineering of the LysR family transcriptional regulator FkbR1 and its target gene to improve ascomycin production. Appl Microbiol Biotechnol 2017;101:4581–92. https://doi.org/10.1007/s00253-017-8242-4.

[23] Kitani S, Ikeda H, Sakamoto T, Noguchi S, Nihira T. Characterization of a regulatory gene, aveR, for the biosynthesis of avermectin in *Streptomyces avermitilis*. Appl Microbiol Biotechnol 2009;82:1089–96. https://doi.org/10.1007/s00253-008-1850-2.

[24] He W, Lei J, Liu Y, Wang Y. The LuxR family members GdmRI and GdmRII are positive regulators of geldanamycin biosynthesis in *Streptomyces hygroscopicus* 17997. Arch Microbiol 2008;189:501–10. https://doi.org/10.1007/s00203-007-0346-2.

[25] Wilson DJ, Xue Y, Reynolds KA, Sherman DH. Characterization and analysis of the PikD regulatory factor in the pikromycin biosynthetic pathway of *Streptomyces venezuelae*. J Bacteriol 2001;183:3468–75. https://doi.org/10.1128/jb.183.11.3468-3475.2001.

[26] Niu G, Chater KF, Tian Y, Zhang J, Tan H. Specialised metabolites regulating antibiotic biosynthesis in *Streptomyces* spp. FEMS Microbiol Rev 2016;40:554–73. https://doi.org/10.1093/femsre/fuw012.

[27] Liu W, Zhang Q, Guo J, Chen Z, Li J, Wen Y. Increasing avermectin production in *Streptomyces avermitilis* by manipulating the expression of a novel TetR-family regulator and its target gene product. Appl Environ Microbiol 2015;81:5157–73. https://doi.org/10.1128/aem.00868-15.

[28] Wu P, Chen K, Li B, Zhang Y, Wu H, Chen Y, et al. Polyketide starter and extender units serve as regulatory ligands to coordinate the biosynthesis of antibiotics in *Actinomycetes*. mBio 2021;12:e0229821. https://doi.org/10.1128/mBio.02298-21.

[29] Mittal M, Singh AK, Kumaran S. Structural and biochemical characterization of ligand recognition by CysB, the master regulator of sulfate metabolism. Biochimie 2017;142:112–24. https://doi.org/10.1016/j.biochi.2017.08.011.

[30] Giannopoulou EA, Senda M, Koentjoro MP, Adachi N, Ogawa N, Senda T. Crystal structure of the full-length LysR-type transcription regulator CbnR in complex with promoter DNA. FEBS J 2021;288:4560–75. https://doi.org/10.1111/febs.15764.

[31] Zhang XS, Luo HD, Tao Y, Wang YY, Jiang XH, Jiang H, et al. FkbN and Tcs7 are pathway-specific regulators of the FK506 biosynthetic gene cluster in *Streptomyces tsukubaensis* L19. J Ind Microbiol Biotechnol 2016;43:1693–703. https://doi.org/10.1007/s10295-016-1849-0.

[32] McClure SM, Ahl PL, Blue JT. High throughput differential scanning fluorimetry (DSF) formulation screening with complementary dyes to assess protein unfolding and aggregation in presence of surfactants. Pharm Res (N Y) 2018;35:81. https://doi.org/10.1007/s11095-018-2361-1.

[33] Zhang Y, Pan G, Zou Z, Fan K, Yang K, Tan H. JadR*-mediated feed-forward regulation of cofactor supply in jadomycin biosynthesis. Mol Microbiol 2013;90:884–97. https://doi.org/10.1111/mmi.12406.

[34] Li Y, Li J, Tian Z, Xu Y, Zhang J, Liu W, et al. Coordinative modulation of chlorothricin biosynthesis by binding of the glycosylated intermediates and end product to a responsive regulator ChlF1. J Biol Chem 2016;291:5406–17. https://doi.org/10.1074/jbc.M115.695874.

[35] Hesketh A, Sun J, Bibb M. Induction of ppGpp synthesis in *Streptomyces coelicolor* A3(2) grown under conditions of nutritional sufficiency elicits actII-ORF4 transcription and actinorhodin biosynthesis. Mol Microbiol 2001;39:136–44. https://doi.org/10.1046/j.1365-2958.2001.02221.x.

[36] Uguru GC, Stephens KE, Stead JA, Towle JE, Baumberg S, McDowall KJ. Transcriptional activation of the pathway-specific regulator of the actinorhodin biosynthetic genes in *Streptomyces coelicolor*. Mol Microbiol 2005;58:131–50. https://doi.org/10.1111/j.1365-2958.2005.04817.x.

[37] Alanazi AM, Neidle EL, Momany C. The DNA-binding domain of BenM reveals the structural basis for the recognition of a T-N11-A sequence motif by LysR-type transcriptional regulators. Acta Crystallogr D Biol Crystallogr 2013;69:1995–2007. https://doi.org/10.1107/s0907444913017320.

[38] Wang W, Wu H, Xiao Q, Zhou H, Li M, Xu Q, et al. Crystal structure details of *Vibrio fischeri* DarR and mutant DarR-M202I from LTTR family reveals their activation mechanism. Int J Biol Macromol 2021;183:2354–63. https://doi.org/10.1016/j.ijbiomac.2021.05.186.